

JGR Solid Earth

RESEARCH ARTICLE

10.1029/2022JB024747

Key Points:

- We have developed the potential field imaging theory to estimate the depth of current sources in *Mise-à-la-masse* surveys
- Synthetic and field applications of a landfill leakage is demonstrated
- An Open-source code for inversion of voltage using potential field imaging theory is provided

Supporting Information:

Supporting Information may be found in the online version of this article.

Correspondence to:

B. Mary,
benjamin.mary@unipd.it

Citation:

Mary, B., Peruzzo, L., Wu, Y., & Cassiani, G. (2022). Advanced potential field analysis applied to *Mise-à-la-masse* surveys for leakage detection. *Journal of Geophysical Research: Solid Earth*, 127, e2022JB024747. <https://doi.org/10.1029/2022JB024747>

Received 11 MAY 2022

Accepted 7 NOV 2022

Author Contributions:

Conceptualization: Benjamin Mary, Luca Peruzzo, Yuxin Wu, Giorgio Cassiani

Data curation: Benjamin Mary, Luca Peruzzo, Giorgio Cassiani

Formal analysis: Benjamin Mary

Funding acquisition: Giorgio Cassiani

Investigation: Giorgio Cassiani

Methodology: Benjamin Mary, Luca Peruzzo, Yuxin Wu

Project Administration: Giorgio Cassiani

Software: Benjamin Mary, Luca Peruzzo

Supervision: Yuxin Wu, Giorgio Cassiani

Validation: Luca Peruzzo

© 2022 The Authors.

This is an open access article under the terms of the [Creative Commons Attribution-NonCommercial License](https://creativecommons.org/licenses/by-nc/4.0/), which permits use, distribution and reproduction in any medium, provided the original work is properly cited and is not used for commercial purposes.

Advanced Potential Field Analysis Applied to *Mise-à-la-Masse* Surveys for Leakage Detection

Benjamin Mary^{1,2} , Luca Peruzzo² , Yuxin Wu² , and Giorgio Cassiani¹ 

¹Dipartimento di Geoscienze, Università degli Studi di Padova, Padova, Italy, ²Earth and Environmental Sciences Area, Lawrence Berkeley National Laboratory, Berkeley, CA, USA

Abstract Traditionally interpretation of *Mise-à-la-masse* (MALM) is limited to the visualization of equipotential contours in order to infer qualitatively the extent of the anomaly. MALM inversion algorithms rely on having a good knowledge of the electrical resistivity distribution in the subsoil. Conversely, potential imaging methods have shown their strength for several applications to quickly estimate the depth of sources even in highly heterogeneous media. In the case of the MALM method, the physics may be described by Poisson's equation. As the conductivity term is modulating the flux of current, MALM is generally referred to as a pseudo-potential method. In this work, we have tested, for the first time, the application of the potential field theory to MALM in order to identify the current source depth. Synthetic modeling shows that the proposed algorithm is effective and efficient, using surface voltage measurements for different resistivity contrasts, anomaly depths and noise levels. We then applied the method to the real field case of a landfill leakage and showed how very different source depth estimates result from an intact or a damaged landfill liner.

Plain Language Summary The so-called *Mise-à-la-Masse* (MALM) technique is a well-known active geoelectrical prospecting method aimed at imaging (qualitatively) electrically conductive (often ore) bodies in the subsurface. The current is injected in the core of the body to prospect, and the high electrical conductivity of the body channels the current making it detectable from the anomalies of electrical potential measured, for example, at the ground surface. Verification of landfill liner integrity is one of the most recent applications of MALM, exploiting the electrical and hydraulic separation, often made with a plastic liner, between the conductive waste inside and the soil outside. Holes in the liner may be imaged inducing a passage of direct current (DC) between the inner and the outer part of the landfill, provided that the location of such holes be identified using an efficient MALM inversion. For this purpose, we adapted an algorithm used for voltage inversion to MALM: the approach has proven effective using synthetic modeling and was successfully applied to real field data from an industrial landfill.

1. Introduction

The *Mise-à-la-Masse* (MALM) method is a variation of the classical geo-electrical investigation approaches, in which direct current (DC) is injected into the ground by two electrodes and the difference is measured between two other points. MALM was originally developed to delineate the shape of electrically conductive mineral bodies for mining exploration purposes (Parasnis, 1967; Schlumberger, 1920). MALM traditional implementation assumes that the conductive (ore) body channels current in such an effective manner so that the characteristics of the surrounding medium are irrelevant and interpretation can be limited to the qualitative shape of the voltage map distribution, the contour isolines giving an estimate of the anomaly extent and orientation. This classic MALM approach has found different applications in recent times, in situations where it is useful to verify the electrical connection between one portion and another of the subsoil (e.g., De Carlo et al., 2013; Mary et al., 2018, 2020; Perri et al., 2018; Peruzzo et al., 2020). The MALM approach holds under the assumptions that the contrast between the conductive body and the background is high and that the conductive body is accessible and has a relatively large volume. Applications at landfill bodies are of particular interest where the aim is to verify the connection between the inside and outside of the waste mass, for example, in presence of a plastic liner which represents, when undamaged, both a hydraulic and an electrical barrier. In this type of application, the interpretation of MALM data is often non-trivial and requires modeling of DC current flow and a reconstruction of the, often poorly known, subsoil heterogeneities. A number of different approaches have been proposed and used to this end, in particular in search for the depth of localized anomaly sources (Binley et al., 1999; Ling et al., 2019; Mary et al., 2020; Peruzzo et al., 2020; Shao et al., 2018; Wondimu et al., 2018). A priori information

Writing – original draft: Benjamin Mary

Writing – review & editing: Benjamin Mary, Luca Peruzzo, Yuxin Wu, Giorgio Cassiani

is always needed to guide the result (de Villiers et al., 2019) and a correction for the influence of the resistivity on the current density distribution is needed.

A large body of literature exists regarding potential field imaging using non-iterative (i.e., no inversion in a strict sense) processing, to estimate the location and depth of sources. Up to now, potential field imaging tools have been reserved to passive methods analysis such as self-potential (SP), gravity or magnetic surveys. Patella (1997) formulated an approach to SP data interpretation where the inverse problem is solved using cross-correlation of the field with a scanning source (the electric field generated by an elementary positive charge). Lapenna et al. (2000) applied that approach to outline the SP source geometry and dynamics within a faulted structure. In their review article, Fedi and Pilkington (2012) discuss a number of existing algorithms and note that all such methods have in common two steps: the upward continuation of the field and a depth weighting factor (scaling function) to identify the source location.

The upward continuation of the field is generally performed via Fourier transformation. An alternative powerful approach is the use of Continuous Wavelet Transform (CWT—Abdelrahman et al., 2008; Agarwal & Srivastava, 2009; Bhattacharya & Roy, 1981; Gibert & Pessel, 2001; Srivastava & Agarwal, 2010; Saracco et al., 2004).

Among other algorithms, the so-called Depth from Extreme Points (DEXP—Fedi, 2007; Fedi et al., 2007) has been especially conceived with the possibility of using the field spatial derivatives to improve the resolution and a more accurate weighting law depending on the so-called Structural Index (SI) of the source. An automatic DEXP imaging method independent from the value of the SI of the causative source was also proposed later to add flexibility to the procedure (Abbas & Fedi, 2014; Abbas et al., 2014). More recently, Baniamerian et al. (2016) introduced the compact-DEXP (CDEXP) algorithm for fast modeling the potential field anomaly. The DEXP transformation and the CWT belong to different theories but present some similarities (Fedi & Pilkington, 2012; Fedi et al., 2010). The key difference between DEXP and CWT is the respective choices of the power-law exponent. In the DEXP case, the exponent depends on the differentiation order and the source properties (through the SI), while in the CWT formulation the exponent depends only on the differentiation order (Revil, 2013). Fedi (2007) discussed the pro and cons of using an imaging against an inversion approach for source depth estimation, since inversion codes of natural potential field also proved their efficiency for spontaneous potential (Soueid Ahmed et al., 2013) and gravity (Fedi, 2007; Florio & Fedi, 2018). Note that Fedi et al. (2010) show that for CWT (and DEXP) the influence of a heterogeneous resistivity distribution (three orders of magnitude differences) is negligible on source depth estimation. As suggested by Liu et al. (2020), the imaged model (using CWT or DEXP) may always be used as a reference or a starting model during a subsequent inversion process.

In this paper we describe a new approach that uses the DEXP theory to interpret MALM surveys to derive approximate source location. The main steps involve (a) synthetic modeling in order to verify to what extent the physics governing MALM is compatible with the potential theory imaging method (reported in the Supporting Information S1); (b) application of the modified DEXP algorithm (in the sequel, named pyDEXP) to a synthetic and a real MALM datasets, both related to the identification of leakage from an industrial landfill.

2. Case Study

The case study we present concerns an industrial landfill in Northern Italy, having the following characteristics:

1. The contaminated part of the site consists of an area of about 2 ha surrounded by a physical barrier, 16 m deep, made of a trench filled with clayey material having an embedded vertical high density polyethylene (HDPE) membrane. The water table is positioned practically at the ground surface. No bottom liner exists.
2. The sediments are silty, saturated by brackish water for which we can assume an electrical conductivity of about 0.5 S/m. Assuming a reasonable formation factor of 5, we expect the saturated formation to have an electrical conductivity of about 0.1 S/m, that is, an electrical resistivity of 10 Ω m.
3. Given the presence of brackish water, one can assume that the resistivity of the entire system, inside and outside the landfill body, is homogeneous and equal to 10 Ω m, with the single most notable exception of the barrier itself, where the HDPE lines corresponds to an exceedingly large resistivity anomaly (Figure 1).

The current injection electrode A was placed 12 m deep in a monitoring borehole inside the landfill (Figure 1). The current return electrode B and the reference voltage electrode N were placed remotely while the rover voltage

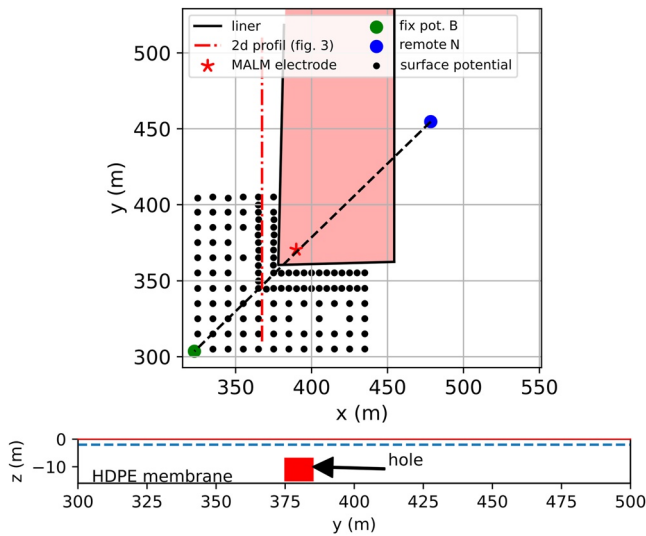


Figure 1. Geometry of the landfill case study: only the South-East corner, around which a leak in the vertical liner was suspected, is sketched here. The inner part of the landfill corresponds to the blurred red area of the figure. Dashed red line show the symmetry of the survey with A, B, and M electrodes aligned. Depth section (yz) showing the possible location and size of the hole (red square) and the position of the water table (dashed blue line).

electrode M was moved on a regular grid of 10×10 m (Figure 1). The fixed electrodes A, B, N all lie on the diagonal of the South-East corner of the landfill (Figure 1): in this way any lack of symmetry of the resulting voltage measured at the ground surface would be indicative of a discontinuity in the HDPE barrier. Note that current can flow anyway from the interior to the exterior of the landfill primarily below the lateral barrier, at a depth of about 16 m from the ground surface, where the HDPE liner ends. Therefore, in absence of any liner discontinuity, the voltage map at the surface should be symmetric with respect to the diagonal of the landfill corner. MALM data were collected in October 2019 using a Syscal Pro (Iris instrument). Both normal and reciprocal configurations (e.g., Binley et al., 1995) were collected in order to ensure optimal data quality. The details of the synthetic modeling for survey design, of data processing and imaging using DEXP are given in the Supporting Information S1.

3. Methods

3.1. Upward Continuation of the Potential Field

The first step common to all potential field processing methods consists in creating a 3D potential field from the data measured along a surface (typically, the ground surface at $z = 0$) and is performed in this study via upward continuation of the surface data u . This is possible because no source of potential field is present above the ground surface. Blakely (1995) formulates the continuation through the Fast Fourier Transform (FFT) in the wave-number domain as:

$$F(U_{up}) = F(u)e^{-\Delta z|k|}, \quad (1)$$

and then transformed back to the space domain. U_{up} is the upward continued data, Δz is the height above the measurement plane, F denotes the Fourier Transform, and $|k|$ is the wavenumber modulus. A particular attention must be given to assigning the right input parameters with regards to the resolution needed, that is, the z discretization.

3.2. Analysis of the Field and Its Derivatives by the DEXP Method

Among all possible ways to analyze the potential field, we propose here an implementation of the DEXP method, as this is flexible enough to estimate source depth density from MALM data and provide a fast image of the source possible distribution. In particular, we take advantage of its automatic SI identification and its good resolution using the derivatives of the potential field.

The final step consists in scaling the field in order to obtain the depth of the source via the DEXP transformation. Fedi (2007) defined the DEXP transformation as:

$$\Omega(r, z_i) = \left| z_i^{\frac{N}{2}} \right| U_{up}(r, z_i) \quad (2)$$

with $i = 1, \dots, L$, and where $\Omega(r, z_i)$ is the DEXP-scaled field at the elevation z_i , $U_{up}(r, z_i)$ is the field u upward continued at z_i (with i being the layer number ranging from 1 to L) and $z_i^{\frac{N}{2}}$ is the DEXP power law. Applying the DEXP transformation to the q th order vertical derivative of the field, results in new DEXP operators (Fedi et al., 2010):

$$\Omega^{(q)}(r, z_i) = \left| z_i^{\frac{(q+N)}{2}} \right| \left. \frac{\partial^q U_{up}(r, z_i)}{\partial z^q} \right|_{z=z_i} \quad (3)$$

and

$$\Omega^{(q)}(r, z_i) = \left| z_i^{\frac{(q+N)}{2}} \left| \frac{\partial^q U_{up}(r, z_i)}{\partial x \partial z^{q-1}} \right|_{z=z_i} \right| \quad (4)$$

with $i = 1, \dots, L$.

Horizontal derivatives can be computed via finite difference or FFT calculation. On the contrary, for stability reasons only FFT can be used for the vertical derivative computation. A set of “ridges” that, according to Fedi's theory (2007), are the extrema of the field and the vertical and horizontal derivatives of the upward continued field are formed. In this study, we refer to ridge types I (RI) and II (RII) respectively where the field horizontal or vertical derivative is zero, and ridge type III (RIII) where the field itself is zero. While it was possible to consider analysis of ridges in order to define the SI (N), we rather implemented the automatic DEXP method (Abbas & Fedi, 2014). The key point in Equation 5 below is that the DEXP ratio R_{mn} is independent of the SI (N) and depends only on known quantities m and n , that is the difference between the orders of the field derivatives f_m and f_n .

$$R_{mn} = \frac{f_m}{f_n} \quad (5)$$

$$\Omega(R_{mn}) = z^{\frac{(m-n)}{2}} R_{mn} \quad (6)$$

3.3. MALM and the Potential Field Theory

In order to process the MALM data, first of all we need to define the physics of the problem. At steady state, the governing partial differential equation (PDE) for the direct current problem is:

$$\nabla \cdot \sigma \nabla V = -I \delta(r) \quad (7)$$

where $\delta(r)$ indicates the Dirac delta positioned at coordinates r and thus indicating point current injection source(s). The voltage in resistivity methods is actually a pseudo-potential since it is modulated by the conductivity σ . If the conductivity of the medium is homogeneous the PDE simplifies to Poisson's equation:

$$\Delta V = I \delta(r) \quad (8)$$

and in absence of current sources to Laplace's equation:

$$\Delta V = 0 \quad (9)$$

The analogy of these equations with those of the gravitational field is, of course, apparent (i.e., given the gravitational potential U , the relevant governing equation is $\Delta U = -4\pi\gamma\rho$ where ρ is density and γ is the gravitational constant). In order to correct for the influence of the return current electrode, thus removing the relevant voltage contribution, we computed this contribution via the simple calculation of the potential V at a point P for a homogeneous soil in a semi-infinite conductor:

$$V(P) = \frac{I}{2\pi l} \quad (10)$$

with I being the intensity of the current injected, and l the distance between the injection point and the point P.

4. MALM Imaging Results on the Landfill

4.1. Voltage Distribution

The resulting voltage distribution in the actual MALM experiment is shown in Figure 2 and compared against the results of the synthetic analog used for survey design (see Supporting Information S1).

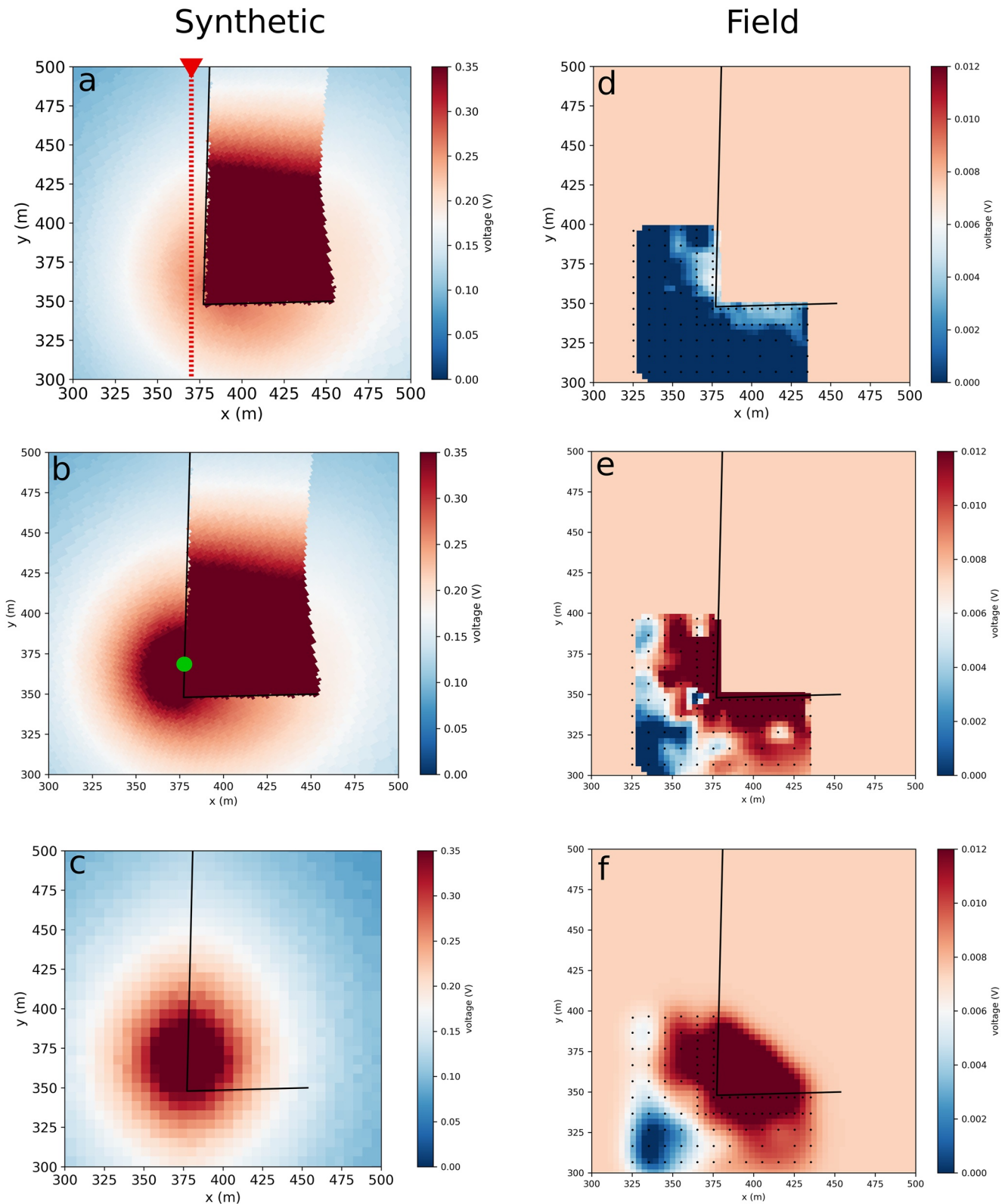


Figure 2. Normalized voltage distribution (voltage/injected current) at the ground surface for synthetic data (left column) and field data (right column). (a and b) Show respectively the simulated normalized voltage for an intact liner and for a perforated liner (the green point indicates the position of a hole 10 m wide and 8 m high, with its top at -12.5 m from the ground), and (c) after mirroring (section Supporting Information S1). (d and e) Show the raw data for the field case respectively before (d), after (e) correction for the influence of the return electrode, and (f) after correction for $B +$ Gaussian smoothing (see Supporting Information S1). The red dashed line indicate the profile used for the DEXP analysis in Figure 3.

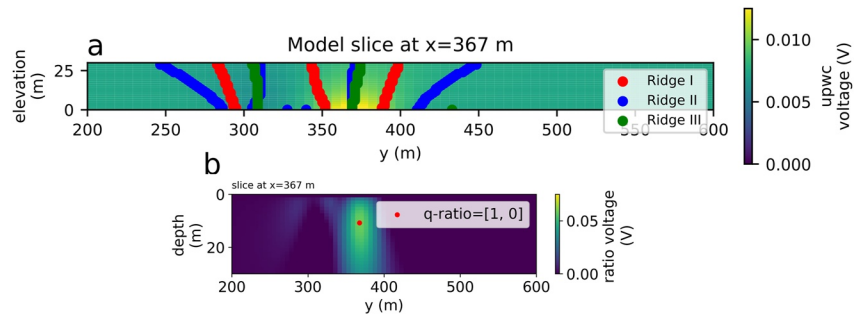


Figure 3. (a) Upward continued section of the field data and its ridges lines from searches for zeros of ridges RI, RII, and RIII (see Supporting Information S1). (b) Depth from Extreme Points transformation using the automatic ratio method between the derivative of order 1 and 0; the maximum (red dot) indicates the source depth estimate.

The simulated voltage for the synthetic case clearly shows how the presence of a discontinuity in the HDPE vertical liner is visible in terms of voltage distribution on the ground surface (compare Figures 2a and 2b). In the simulations the hole is 10 m wide and 8 m high, and its top is at 12.5 m depth from the ground surface.

Figure 2c shows the synthetic results for the damaged liner case after mirroring (see Supporting Information S1 for details) along the line parallel to the Southern border of the landfill (see Figure 1). The procedure is needed in order to confirm the data (available in practice only outside of the landfill) with the theory that is designed to look for a point-like anomaly along a vertical plane of symmetry.

As for the field data, a comparison between Figures 2d and 2e shows how the correction for the influence of the current return electrode location changes the pattern and the amplitude of the normalized voltage distribution. After correction, the field data show with more evidence that the anomaly of electrical potential propagates outside the landfill area. Similar to the synthetic data, mirroring of the field data around the landfill lateral wall is needed for multi-ridge analysis as described in the DEXP approach (Figure 2f).

4.2. Estimation of Leak Point From Field Data

The multi-ridge analysis in the DEXP approach is designed to identify the location of the source at depth. We conducted such an analysis using the MALM voltages collected during the field survey in a totally analogous manner as for the synthetic data described in the Supporting Information S1. The analysis is conducted in 2D along the line of Southern side of the landfill (Figure 1). However, for the field data, many ridges appeared to be inconsistent disturbing their intersections. We cannot reach conclusions concerning the source depth based only on the geometrical analysis of the ridge intersections. However, the ratio DEXP analysis shows the source at approximately 8 m depth (Figure 3).

5. Discussion

The use of the potential field imaging theory for the identification of MALM source depth due to current leakage (in the specific case, from a landfill) has pros and cons. When applied to passive prospecting methods (such as SP or gravimetry), potential methods seek for a naturally induced source at depth. Conversely, in the MALM case, the field is induced by current injection via a pair of electrodes. The current propagates through the conductive body and is then diffused to the soil. In this study the position of the current electrode was placed very close to the leakage point. The conductive nature of the inner landfill material reduces the effect of the actual location of the current location point, and conveys current toward the leak. The source producing the electrical potential is thus linked to the current circulation in the conductive body. As the MALM assumption relies on the fact that the conductive body is much more conductive with respect to the surrounding medium, we tested this assumption against the potential field imaging theory. Note that our MALM approach is aimed at identifying the source not the conductive body extent.

The location of the MALM (A) electrode far from the leakage point would lead to a wrong estimate of the leak position. When moving A, most of the current spreads out under the liner instead of going through the hole

(figure not shown). The potential field distribution is alike to a no-hole configuration and applying the DEXP procedure results in a wrong estimate of the depth. Considering the complex geometry of the landfill, a 3d DEXP analysis would help to identify the source position and depth. Indeed, running a 3d analysis would allow better discrimination between the residual background signal due to the current going under the landfill and the current going into the hole.

Here for simplicity and by lack of data, although most likely the subsurface was heterogeneous due to highly conductive leachates relative to surrounding groundwater, we assumed an homogeneous soil during the correction of the influence of the electrode N position. In a preliminary study we found that the effect of the initial resistivity model that is, the contrast of conductivity between the body and its surrounding medium does not affect the source depth position identification up to three orders of magnitude differences (see Supporting Information S1). This is in-line with Mauri et al. (2010) who show a similar result for the CWT case applied to SP signals (i.e., also conditioned by the electrical resistivity distribution). Also varying the noise level and source depth showed respectively no effect and small errors on the source depth detection using the DEXP ratio analysis.

An important limiting factor of the potential field theory is the choice of the SI matching the anomaly shape (Stavrev & Reid, 2007) which ultimately guides the choice of the depth weighting factor. This can be very difficult to assess in complex field sites. In the case of a landfill leakage, however, this is a minor problem as the anomaly can be considered point-like and isolated. This could explain why for the synthetic cases the estimated source parameters show very good agreement with the “true” values (both for gravimetric and MALM data—see Supporting Information S1).

An important issue to consider relates to the presence of domain boundaries. In a simple case, the only electrical boundary to consider is the soil/air interface. In the specific case of the described landfill, it is necessary to deal with the liner boundary. We removed the influence of the liner boundary by mirroring the data around the boundary before applying the upward continuation of the field. The outside part of the landfill was mirrored against a line parallel to the landfill side. The step is validated via synthetic modeling (see Supporting Information S1 material) where the source depth was correctly estimated. Correcting for the pole source is most of the time not required for field application of MALM; and in other cases a reasonable estimation of electrical resistivity distribution can be obtained from ERT—in this case the correction is not really needed due to the homogenizing effect of the brackish water high electrical conductivity. Note that the survey described in this paper was likely the most penalizing case that we could encounter for leakage detection: for some cases the landfill is accessible and the remote electrode can be placed far away to avoid the correction step. For these other easier cases less refined strategies shall be applied.

This study shows that the estimation of source locations can be biased by a few factors, and in particular: (a) the quality of the data (b) the stability of the upward continuation and of its spatial derivatives. About these factors, first of all, we note that the noise is confined to low elevations, due to the well-known smoothing effect of the upward continuation operator in the DEXP transformation. This noise was successfully removed fitting the ridges to a given range of altitudes. While an efficient way to isolate the anomalies is to vary the order of the differentiation of the field (which can be safely done thanks to the smoothing properties of the upward continuation), in this study the anomaly was easily identified only using the ratio between the first and the upward continued field.

This approach overcomes some limitations of the classical inversion, yet potential field methods are subject to bias just like any other geophysical inverse problem. The potential field imaging of MALM does not converge perfectly to the exact location of sources if the resistivity model is very complex. At most, an approximate (and yet very useful) source location is identified. This is expected consistently with literature evidence. The best approach that can limit the natural uncertainty in source identification is the use of synthetic modeling, based on solid assumptions concerning the expected anomalies distributions and source locations. The results of these exercises become fundamental in supporting the interpretation of the MALM results.

6. Conclusions

This study presents a successful application of MALM, a well-established geo-electrical method, using a novel processing approach. The information content of MALM is fully exploited using the potential field imaging theory. The results we present are relevant to both a synthetic study and a field case. The synthetics indicate that the proposed approach can estimate the source depth accurately considering a correction of the influence

of the remote current return electrode. The field application exploited the theory to estimate the leak depth from a damaged landfill. Synthetic modeling reproducing the actual field conditions shows that an hole into the liner where the current can leak can be seen both from the multi-ridge analysis and DEXP. For the real case, the source depth analysis shows similar results than the damaged synthetic modeling.

Data Availability Statement

Codes and data to reproduce figures articles are available in the Zenodo data repository (<https://doi.org/10.5281/zenodo.6538070>) and in to the Github (https://github.com/BenjMy/dEXP_imaging/tree/master/notebooks_JGR).

Acknowledgments

The authors thank L. Slater and the anonymous reviewers for their constructive comments on the manuscript. This project has received funding from the European Union's Horizon 2020 research and innovation programme under the Marie Skłodowska-Curie grant agreement No 842922. The authors acknowledge financial support from the Italy-Israel bilateral project ECZ-Dry.

References

- Abbas, M. A., & Fedi, M. (2014). Automatic DEXP imaging of potential fields independent of the structural index. *Geophysical Journal International*, 199(3), 1625–1632. <https://doi.org/10.1093/gji/ggu354>
- Abbas, M. A., Fedi, M., & Florio, G. (2014). Improving the local wavenumber method by automatic DEXP transformation. *Journal of Applied Geophysics*, 111, 250–255. <https://doi.org/10.1016/j.jappgeo.2014.10.004>
- Abdelrahman, E. M., El-Araby, T. M., Abo-Ezz, E. R., Soliman, K. S., & Essa, K. S. (2008). A new algorithm for depth determination from total magnetic anomalies due to spheres. *Pure and Applied Geophysics*, 165(5), 967–979. <https://doi.org/10.1007/s00024-008-0340-x>
- Agarwal, B. N. P., & Srivastava, S. (2009). Analyses of self-potential anomalies by conventional and extended Euler deconvolution techniques. *Computers & Geosciences*, 35(11), 2231–2238. <https://doi.org/10.1016/j.cageo.2009.03.005>
- Baniamerian, J., Fedi, M., & Oskooi, B. (2016). Research note: Compact depth from extreme points: A tool for fast potential field imaging: Compact depth from extreme points. *Geophysical Prospecting*, 64(5), 1386–1398. <https://doi.org/10.1111/1365-2478.12365>
- Bhattacharya, B. B., & Roy, N. (1981). A note on the use of a nomogram for self-potential anomalies. *Geophysical Prospecting*, 29(1), 102–107. <https://doi.org/10.1111/j.1365-2478.1981.tb01013.x>
- Binley, A., Daily, W., & Ramirez, A. (1999). Detecting leaks from waste storage ponds using electrical tomographic methods (Vol. 8).
- Binley, A., Ramirez, A., & Daily, W. (1995). Regularised image reconstruction of noisy electrical resistance tomography data. In *Proceedings of the 4th workshop of the European concerted action on process tomography* (pp. 401–410).
- Blakely, R. J. (1995). *Potential theory in gravity and magnetic applications*. Cambridge University Press. <https://doi.org/10.1017/CBO9780511549816>
- De Carlo, L., Perri, M. T., Caputo, M. C., Deiana, R., Vurro, M., & Cassiani, G. (2013). Characterization of a dismissed landfill via electrical resistivity tomography and mise-à-la-masse method. *Journal of Applied Geophysics*, 98, 1–10. <https://doi.org/10.1016/j.jappgeo.2013.07.010>
- de Villiers, G., Ridley, K., Rodgers, A., & Boddice, D. (2019). On the use of the profiled singular-function expansion in gravity gradiometry. *Journal of Applied Geophysics*, 170, 103830. <https://doi.org/10.1016/j.jappgeo.2019.103830>
- Fedi, M. (2007). DEXP: A fast method to determine the depth and the structural index of potential fields sources. *Geophysics*, 72(1), I1–I11. <https://doi.org/10.1190/1.2399452>
- Fedi, M., Cella, F., Quarta, T., & Villani, A. V. (2010). 2D continuous wavelet transform of potential fields due to extended source distributions. *Applied and Computational Harmonic Analysis*, 28(3), 320–337. <https://doi.org/10.1016/j.acha.2010.03.002>
- Fedi, M., Florio, G., & Cascone, L. (2007). *Improved SCALFUN analysis of potential fields by a criterion of ridge-consistency*. European Association of Geoscientists & Engineers. <https://doi.org/10.3997/2214-4609.201401601>
- Fedi, M., & Pilkington, M. (2012). Understanding imaging methods for potential field data. *Geophysics*, 77(1), G13–G24. <https://doi.org/10.1190/geo2011-0078.1>
- Florio, G., & Fedi, M. (2018). Depth estimation from downward continuation: An entropy-based approach to normalized full gradient. *Geophysics*, 83(3), J33–J42. <https://doi.org/10.1190/geo2016-0681.1>
- Gibert, D., & Pessel, M. (2001). Identification of sources of potential fields with the continuous wavelet transform: Application to self-potential profiles. *Geophysical Research Letters*, 28(9), 1863–1866. <https://doi.org/10.1029/2000GL012041>
- Lapenna, V., Patella, D., & Piscitelli, S. (2000). Tomographic analysis of self-potential data in a seismic area of southern Italy. *Annali di Geofisica*, d3, 361–373.
- Ling, C., Revil, A., Qi, Y., Abdulsamad, F., Shi, P., Nicaise, S., & Peyras, L. (2019). Application of the Mise-à-la-Masse method to detect the bottom leakage of water reservoirs. *Engineering Geology*, 261, 105272. <https://doi.org/10.1016/j.enggeo.2019.105272>
- Liu, S., Baniamerian, J., & Fedi, M. (2020). Imaging methods versus inverse methods: An option or an alternative? *IEEE Transactions on Geoscience and Remote Sensing*, 58(5), 3484–3494. <https://doi.org/10.1109/TGRS.2019.2957412>
- Mary, B., Peruzzo, L., Boaga, J., Cenni, N., Schmutz, M., Wu, Y., et al. (2020). Time-lapse monitoring of root water uptake using electrical resistivity tomography and mise-à-la-masse: A vineyard infiltration experiment. *SOIL*, 6(1), 95–114. <https://doi.org/10.5194/soil-6-95-2020>
- Mary, B., Peruzzo, L., Boaga, J., Schmutz, M., Wu, Y., Hubbard, S. S., & Cassiani, G. (2018). Small-scale characterization of vine plant root water uptake via 3-D electrical resistivity tomography and mise-à-la-masse method. *Hydrology and Earth System Sciences*, 22(10), 5427–5444. <https://doi.org/10.5194/hess-22-5427-2018>
- Mauri, G., Williams-Jones, G., & Saracco, G. (2010). Depth determinations of shallow hydrothermal systems by self-potential and multi-scale wavelet tomography. *Journal of Volcanology and Geothermal Research*, 191(3), 233–244. <https://doi.org/10.1016/j.jvolgeores.2010.02.004>
- Parasnis, D. S. (1967). Three-dimensional electric mise-à-la-masse survey of an irregular lead-zinc-copper deposit in central Sweden. *Geophysical prospecting* (Vol. 15, pp. 407–437). European Association of Geoscientists & Engineers. <https://doi.org/10.1111/j.1365-2478.1967.tb01796.x>
- Patella, D. (1997). Introduction to ground surface self-potential tomography. *Geophysical Prospecting*, 45(4), 653–681. <https://doi.org/10.1046/j.1365-2478.1997.430277.x>
- Perri, M. T., De Vita, P., Masciale, R., Portoghesi, I., Chirico, G. B., & Cassiani, G. (2018). Time-lapse Mise-à-la-Masse measurements and modeling for tracer test monitoring in a shallow aquifer. *Journal of Hydrology*, 561, 461–477. <https://doi.org/10.1016/j.jhydrol.2017.11.013>
- Peruzzo, L., Chou, C., Wu, Y., Schmutz, M., Mary, B., Wagner, F. M., et al. (2020). Imaging of plant current pathways for non-invasive root Phenotyping using a newly developed electrical current source density approach. *Plant and Soil*, 450(1–2), 567–584. <https://doi.org/10.1007/s11104-020-04529-w>

- Revil, A. (2013). Comment on "A fast interpretation of self-potential data using the depth from extreme points method" (M. Fedi and M. A. Abbas, 2013, *Geophysics*, 78, no. 2, E107–E116). *Geophysics* (Vol. 78, pp. X1–X7). Publisher: Society of Exploration Geophysicists. <https://doi.org/10.1190/geo2013-0052.1>
- Saracco, G., Labazuy, P., & Moreau, F. (2004). Localization of self-potential sources in volcano-electric effect with complex continuous wavelet transform and electrical tomography methods for an active volcano. *Geophysical Research Letters*, 31(12), L12610. <https://doi.org/10.1029/2004GL019554>
- Schlumberger, C. (1920). *Étude sur la prospection électrique du sous-sol*. Gauthier-Villars.
- Shao, Z., Revil, A., Mao, D., & Wang, D. (2018). Finding buried metallic pipes using a non-destructive approach based on 3D time-domain induced polarization data. *Journal of Applied Geophysics*, 151, 234–245. <https://doi.org/10.1016/j.jappgeo.2018.02.024>
- Soueid Ahmed, A., Jardani, A., Revil, A., & Dupont, J. (2013). SP2DINV: A 2D forward and inverse code for streaming potential problems. *Computers & Geosciences*, 59, 9–16. <https://doi.org/10.1016/j.cageo.2013.05.008>
- Srivastava, S., & Agarwal, B. N. P. (2010). Inversion of the amplitude of the two-dimensional analytic signal of the magnetic anomaly by the particle swarm optimization technique: Inversion of AAS by PSO. *Geophysical Journal International*, 182(2), 652–662. <https://doi.org/10.1111/j.1365-246X.2010.04631.x>
- Stavrev, P., & Reid, A. (2007). Degrees of homogeneity of potential fields and structural indices of Euler deconvolution. *Geophysics* (Vol. 72, pp. L1–L12). Publisher: Society of Exploration Geophysicists. <https://doi.org/10.1190/1.2400010>
- Wondimu, H. D., Mammo, T., & Webster, B. (2018). 3D joint inversion of Gradient and Mise-à-la-Masse borehole IP/Resistivity data and its application to magmatic sulfide mineral deposit exploration. *Acta Geophysica*, 66(5), 1031–1045. <https://doi.org/10.1007/s11600-018-0199-x>